

# Seismic Assessment of Innovative Hybrid Bracing System Equipped with Shape Memory Alloy

**A. Jalaeefer & B. Asgarian**

*Civil Engineering faculty, K.N. Toosi University of Technology, Iran*



## **SUMMARY:**

The usage of special braces has increased since the 1994 Northridge Earthquake. Past performances suggest limited energy dissipation and ductility in braces due to buckling. To overcome these limitations, a hybrid seismic brace equipped with shape memory alloy that provides both energy-absorbing and re-centering capabilities is developed and evaluated and its seismic performance is compared to traditional braces. SMA is a unique metallic alloy that has the ability to undergo large deformations while reverting back to its original undeformed shape providing re-centering capabilities to the brace. Detailed analytical finite element models of ordinary and hybrid braces are developed and cyclic loading histories are used to evaluate their efficiency in seismic loads. Results suggest that the hybrid bracing system is effective in limiting residual deformations during an earthquake, due to the re-centering nature of super-elastic SMA.

*Keywords: shape memory alloy, energy dissipating, re-centering, hybrid, Nitinol*

## **1. INTRODUCTION**

Although there has been an increase in the use of CBF systems, damage during past earthquakes suggests that braced systems may perform poorly due to limited ductility and energy dissipation, failure of the connection between the braces and the frame, and asymmetric behavior of the brace in tension and compression.

One way of improving the performance of CBF systems in terms of limiting inter-story drifts is the use of innovative materials in the bracing system. In particular, super-elastic shape memory alloys (SMAs) have been shown to develop a flag-shape hysteresis under cyclic axial loading, which can provide both re-centering and supplemental energy dissipation to a structural system, which results in limiting inter-story drifts and decreasing permanent displacement of the structure. But previous studies imply that the amount of energy dissipated in one loading cycle of SMA is less than the similar amount for mild structural steel. Besides, SMA is an almost expensive material compared to steel. Thus it does not seem reasonable to substitute the whole section area of a bracing member with shape memory alloy.

The objective of this study is to assess the performance of a hybrid damping device with parallel usage of steel and SMA for use in bracing members. Achieving the optimum proportion of SMA to steel in the brace section area in addition to proposing a practical and simple detail for the hybrid device are the other goals of the present study. Cyclic dissipated energy and the residual plastic strains of dampers with various SMA/Steel proportions are estimated to determine the potential of using the device along with a rigid brace. This will localize the energy absorbing and re-centering characteristics in addition to minimizing the amount of SMA used.

## 1.1. Shape memory alloy

SMA are metallic materials which can undergo large deformations (strains up to 10%) while recovering their initial configuration, without almost any residual deformation, at the end of cyclic loading. This is a result of martensitic phase-transformation which can be either temperature induced or stress induced. Shape memory alloys are two-phase metals that may exist either in austenitic or in martensitic form. The former has a stiffer metallographic structure that gives rise to high yield strength, while the latter exhibits lower yield and is less rigid. Depending on the material temperature (greater or lower than austenitic finish temperature  $A_f$ ) shape memory alloys exhibit two different mechanical properties. If the temperature is greater than  $A_f$ , strains attained on loading are completely recovered after unloading (Figure1). This process leads to significant energy-absorbing capacity with zero residual strain and is called super-elasticity.

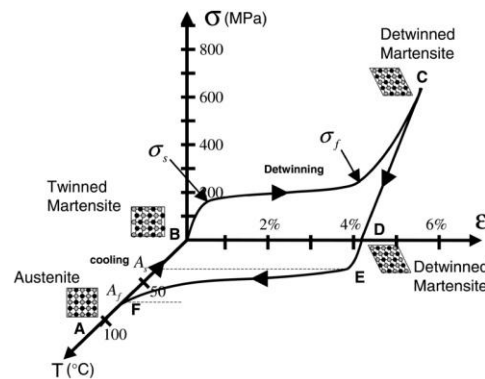


Figure 1. A typical SMA super-elastic loading cycle [Lagoudas D]

## 1.2. Previous studies on the usage of SMA in structures

Recent interest in the development of new technologies to limit inter-story and residual drifts in civil engineering structures as a result of a seismic event has led to several numerical and experimental studies which have highlighted the possibility of utilizing SMAs as a promising innovative material for the dynamic control of buildings. The use of super-elastic SMA bars as restrainers was studied by Andrawes and DesRoches [2005] to prevent unseating of the bridge deck from the pier. The re-centering capability and high fatigue-resistance of SMAs has led to studies on their use in cable stay bridge systems [Li et al. 2004]. The investigation of a combined cable-SMA damper system showed an ability of the SMA damper to suppress cable vibration in dominant modes depending on the position of the damper along the cable. Along with the use of SMAs in bridge systems, there have been a significant number of developments involving the use of SMAs in building structures. A more recent study by Masuda et al. [2004] analytically looked at isolation devices using SMA wires to provide energy dissipation. Besides isolation systems and those more innovative strategies presented, bracing systems have been one of the more common areas where the use of SMAs has been considered for frame structures. More recently, studies by Baratta and Corbi [2002] and Han et al. [2003] determined the effectiveness of SMA braces in a simple portal frame and a small scale two-story structure, respectively. Speicher et al. [2008] proposed a tension compression device composed of SMA springs to be used in bracing members. McCormick et al. [2007] studied seismic behavior of CBF systems equipped with SMA braces. They used rigid bracing members with pure SMA, no steel, at both ends. The result of their study is the motivation for the present research [DesRoches, R., 2010]. DesRoches et al. [2010] proposed a hybrid tension-compression device composed of shape memory alloy wires.

In this study a hybrid steel-SMA device composed of shape memory alloy bars is proposed.

## 2. DESCRIPTION OF MODELED DAMPERS

A total of 8 various hybrid dampers are modeled with different SMA/steel proportions to evaluate the parallel combination of the two materials. Detailed finite element models are developed in ANSYS finite element environment.

### 2.1. Hybrid device geometry

Details of the proposed hybrid device for use in a brace member are illustrated in figure 2. As shown, each damper is made up of two thick and rigid plates at each end which are connected to each other using 1, 3 or 5 bars of 8mm diameter. These bars are made up of structural steel or shape memory alloy with various proportions in each damper and are the main load resisting elements of the device. To take advantage of these slender bars in compression in addition of tension, a high strength cement based grout fills the space around them which prevents buckling. The bars and the grout are placed in a thin walled tube providing lateral surrounding pressure for the grout. A 20mm free space remains at each end of the damper which can be filled with a soft non-load bearing substance like polystyrene. In addition the thin walled tube is also welded to only one of the end plates and free at the other end. Thus it is guaranteed that neither the grout, nor the tube will not contribute in axial load resisting of the device and will just prevent the bars from buckling.

### 2.2. Material modeling properties

The two thick end plates of the device can be made up of high strength steel. But in modeling the dampers they are assumed to be elastic with high modules of elasticity.

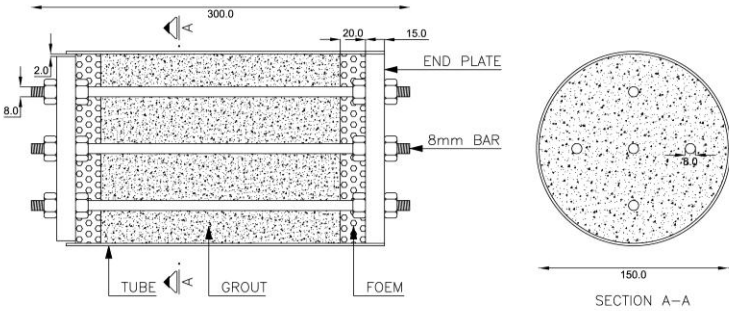


Figure 2. Hybrid device details

Thus their probable deformations will not affect the overall behavior of the damper and they uniformly distribute applied loads or displacements between the main bars. On the other hand, the main bars of the dampers are made up of either St-37 steel or Nitinol shape memory alloy. St-37 steel is modeled using a bilinear curve assuming kinematic hardening law. Results of Fugazza (2005) experimental studies on cyclic behavior of Nitinol bars are used for modeling the shape memory alloy's stress strain curve. According to these results, a stress strain curve is assumed and verified for the shape memory alloy bars with the following parameters (Figure 3).

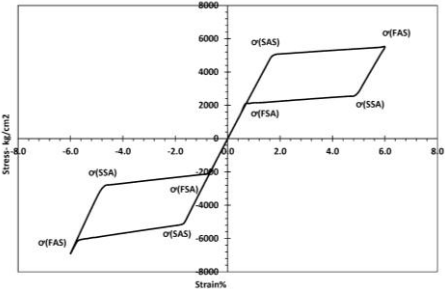


Figure 3. Shape memory alloy stress-strain curve

### 2.3. Definition of modeled dampers

According to the mentioned assumptions, 8 finite element models of different hybrid dampers with various SMA to steel proportions are developed. The first set of dampers are consisted of two different models composed of only one 8mm diameter bar made up of either steel or SMA. The second and the third sets are dampers with three and five bars of the same materials. Table 1 summarizes the details of all dampers with the total number of bars and the number of steel and SMA bars and their ratio. The definition of dampers is based on the SMA to steel ratio to obtain the optimum proportion. Figure 4 shows finite element model of a 5 bar damper.

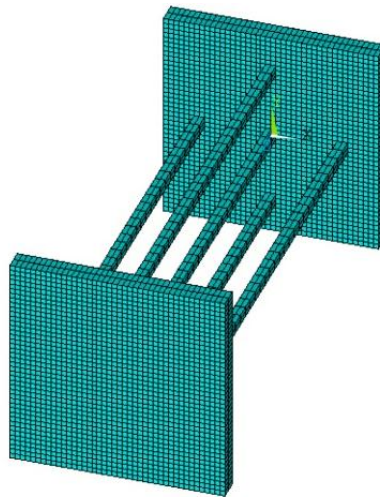


Figure 4. Finite element model of a damper with 5 bars

### 2.4. Modeling, loading and analysis assumptions

Detailed finite element model of each damper is developed in ANSYS finite element program. 8mm diameter section of the bars ( $50.2 \text{ mm}^2$  area) is modeled with an equivalent square of 7mm width ( $49 \text{ mm}^2$  area) for simplicity. Eight node solid elements are used for meshing the volumes and displacement control static analysis is performed assuming large deformation formulation. Lateral high stiffness springs surround each bar representing the cement based grout which prevents the bars from local or global instability.

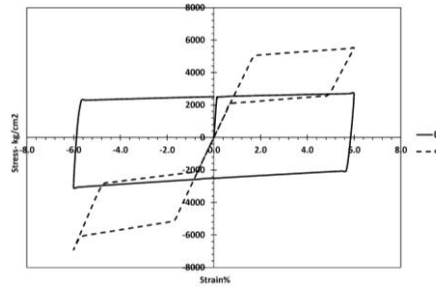
Although SMAs can exhibit re-centering properties for strain values in the 8\_10% range, a conservative value of 6% strain is used herein for two reasons. First, this stricter limit is enforced to avoid the second stiffening phenomenon that can increase SMA stresses from 2 to 5 times the forward transformation stress, which will probably result in a serious damage to the adjacent structural members. Second, this limit is used to retain the re-centering capacity of the SMA bars even after the hybrid device reaches large displacements. Considering this safety margin, each damper is loaded up to 6% both in tension and compression.

## 3. SINGLE BAR DAMPERS

The first set of the samples is composed of two single bar devices, one with an 8mm diameter steel bar (sample S1) and the other with the same size SMA bar (sample S8). These two are the extreme cases of the study with the SMA/steel ratio of '0' and ' $\infty$ ' respectively. Figure 5 illustrates the stress-strain curves of these samples.

**Table 1:** Definition of modeled dampers

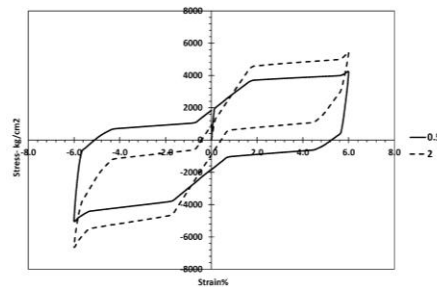
Name of	Total Number of bars	Number of SMA bars	Number of steel bars	SMA/steel Ratio
S1	1	0	1	0.00
S2	5	1	4	0.25
S3	3	1	2	0.50
S4	5	2	3	0.67
S5	5	3	2	1.50
S6	3	2	1	2.00
S7	5	4	1	4.00
S8	1	1	0	$\infty$

**Figure 5.** Stress-strain curves of single bar dampers

As shown in these figures sample S1 with a single steel bar exhibits an open hysteresis curve with maximum area while having a large non-recoverable plastic strain. But sample S8 with a single SMA bar exhibits a double flag shaped hysteresis with minimum area while recovering the strains and having no non-recoverable plastic deformations. The behavior of the bars is almost the same in tension and compression, but due to Poisson's ratio, the section area of the bars decrease in tension (necking) while increasing in compression. Thus compressive stresses are usually a bit larger than tensile stresses in the same strain level.

#### 4. DAMPERS WITH 3 BARS

The second set of the samples is also composed of two dampers with 3 bars having SMA/steel ratios of '0.50' and '2.00'. First with an 8mm diameter SMA bar in the middle and two same sized steel bars at each side (sample S3). The other with the same configuration composed of two SMA bars against one steel bar (sample S6). Figure 6 illustrates the stress-strain curves of these samples.

**Figure 6.** Stress-strain curves of dampers with 3 bars

As shown in these figures sample S3 with SMA/steel ratio of '0.5' exhibits a semi-flag shaped hysteresis curve almost similar to sample S1 with smaller area and less permanent plastic strain. Sample S6 with SMA/steel ratio of '2.00' has a hysteresis almost similar to sample S8 with greater area and more non-recoverable plastic strain as expected.

## 5. DAMPERS WITH 5 BARS

The last set of the samples is composed of four dampers with 5 bars having SMA/steel ratios of '0.25, 0.67, 1.50 and 4.00'. Sample S2 has a single SMA bar surrounded by 4 steel bars. Sample S4 has three steel bars and two SMA bars. Sample S5 has three SMA bars and two steel ones. Sample S7 is composed of a single steel bar surrounded by four SMA ones. Figure 7 illustrates the force-displacement and the stress-strain curves of these samples. As expected, the plastic permanent strain and the area under the stress-strain curves decrease with the increase in SMA/steel ratio. The area under the stress-strain curves represent the amount of dissipated cyclic energy.

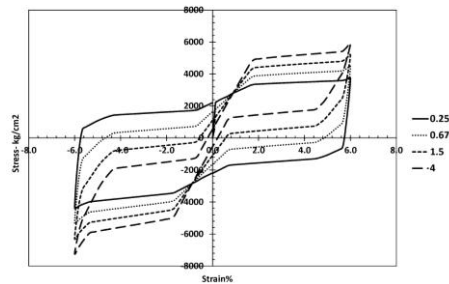


Figure 7. Stress-strain curves of dampers with 5 bars

## 6. PERMANENT PLASTIC STRAIN

Figure 8 illustrates the stress-strain curves of the eight samples in a single diagram. As seen in this figure, the amount of permanent strain decreases as the SMA/steel ratio increases.

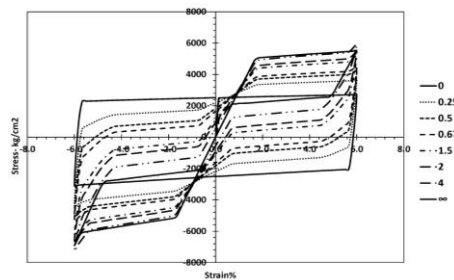
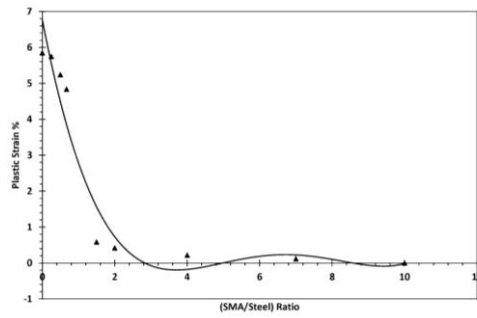


Figure 8. Stress-strain curves for all eight dampers

The amounts of permanent strains of all eight samples in first tensile cycle are summarized in table 2. Figure 9 shows these amounts against SMA/steel ratio with an approximate trend line.

Table 2. Permanent plastic strain and dissipated cyclic energy of samples

Name of sample	SMA/steel Ratio	Permanent strain%	Dissipated energy
S1	0.00	5.85	108.58
S2	0.25	5.75	104.07
S3	0.50	5.24	94.18
S4	0.67	4.84	89.23
S5	1.50	0.58	74.37
S6	2.00	0.42	69.41
S7	4.00	0.22	59.49
S8	$\infty$	0	44.39



**Figure 9.** Plastic permanent strain vs. SMA/steel ratio

### 7. DISSIPATED CYCLIC ENERGY

As seen in figure 9, the amount dissipated cyclic energy decreases as the SMA/steel ratio increases and the samples with greater steel/SMA ratio are more effective in dissipating energy. The amounts of dissipated cyclic energy of all eight samples in first tensile cycle are summarized in table 2. Figure 10 shows these amounts against SMA/steel ratio with an approximate trend line.

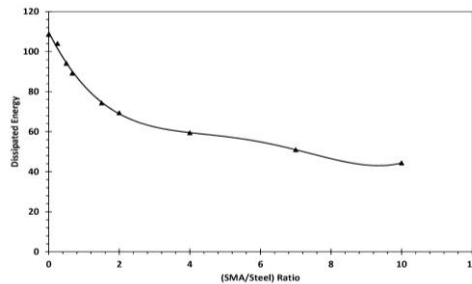


**Figure 10.** Dissipated cyclic energy vs. SMA/steel ratio

### 8. OPTIMUM SMA/STEEL RATIO

The two main factors namely permanent plastic strains and dissipated cyclic energy vary with SMA/steel proportion. If the SMA/steel ratio increases, the permanent plastic strains and the amount of dissipated energy decrease. It is necessary to define an optimum SMA/steel ratio in which both of the two main factors would have a reasonable and acceptable amount. To achieve this goal the amount of recoverable strain (elastic strain) for each sample is plotted in figure 11 against dissipated cyclic energy. Both parameters are normalized using the maximum values to make the comparison possible. The amounts of dissipated energy are normalized with the dissipated energy of sample S1 and the recoverable strains are normalized with the maximum 6% strain. Recoverable strain,  $\epsilon_r$ , is the recovered strain after unloading the device (Table 2).

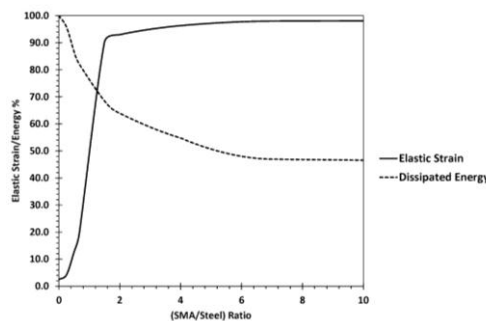


**Figure 11.** Optimum SMA/steel ratio

The intersection of the two curves is the optimum point in which both dissipated energy and permanent plastic strain are maximized simultaneously. This occurs in a SMA/steel ratio of about '1.25'. In this point more than 70% of total strain is recoverable while the dissipated energy ratio against structural steel is also more than 70%. Thus taking advantage of shape memory alloy parallel with structural steel leads to better performance of the device both in recovering the strains and dissipating the earthquake energy. This will not be achieved if each of the materials is used without the other.

## 9. CONCLUSIONS AND SUGGESTIONS

The following conclusions are drawn based on the results and observations presented herein.

- a. When using shape memory alloy and steel in a parallel combination, the hybrid devices exhibit both re-centering capacity and energy dissipation.
- b. If the SMA/steel ratio increases, the permanent plastic strains decrease
- c. If the SMA/steel ratio increases, the amount of dissipated energy decreases.
- d. The optimum ratio of shape memory alloy to steel is about '1.25'. Although this varies a little with the change in material properties, but a narrow band between 1 and 1.5 can optimize both energy dissipating and re-centering capacity.
- e. Placing the proposed device in a rigid bracing member will localize the energy absorbing and re-centering characteristics in addition to minimizing the amount of SMA used.

There is a lack of experimental studies in the compressive behavior of shape memory alloys. Also the proposed device is needed to be experimentally evaluated.

## REFERENCES

- Andrewes B, DesRoches R (2007), "Effect of Hysteretic Properties of Super-elastic Shape Memory Alloys on the Seismic Performance of Structures", *Structural Control and Health Monitoring*, 14:301\_20, John Wiley & Sons.
- Asgarian B, Jalaefar A (2009) "Incremental Dynamic Analysis of Steel braced Frames Designed Based on the 1<sup>st</sup>, 2<sup>nd</sup> and 3<sup>rd</sup> Editions of Iranian Seismic Code 2800", *The Structural Design of Tall And Special Buildings-18*, 000-000, John Wiley & Sons.
- Auricchio F, Fugazza D, DesRoches R (2006), "Earthquake Performance of Steel Frames with Nitinol Braces", *Journal of Earthquake Engineering*, Vol. 10, No. 0, pp. 45-66, Taylor & Francis.
- Chuang Sheng, Yang W, DesRoches R, Leon R (2010), "Design and Analysis of Braced Frames with Shape Memory Alloy and Energy-Absorbing Hybrid Devices", *Engineering Structures* 32 498-507. Elsevier Ltd.
- Lagoudas D (2008) "Shape Memory Alloys - Modeling and Engineering Applications" Texas A&M University TX, USA, Springer.
- Dolce M, Cardone D, Marnetto R. (2000) "Implementation and Testing of Passive Control Devices Based on Shape Memory Alloys", *Earthquake Engineering and Structural Dynamics*, 29: 945-68, John Wiley & Sons.
- Fugazza D (2003) "Shape-Memory Alloy Devices for Earthquake Engineering: Mechanical Properties, Constitutive Modeling and Numerical Simulations", Masters' thesis, European School for Advanced Studies in Reduction of Seismic Risk, Pavia, Italy.
- Fugazza D. (2005) "Use of Shape-Memory Alloy Devices in Earthquake Engineering: Mechanical Properties, Advanced Constitutive Modeling and Structural Applications", Ph.D. dissertation, European School for Advanced Studies in Reduction of Seismic Risk. Pavia, Italy.
- Mazzoni S, McKenna F, Scott MH, Fenves GL. (2006) "OpenSees Command Language Manual", Pacific Earthquake Engineering Research Center; Berkeley Edu.
- McCormick J, DesRoches R, Fugazza D, Auricchio F (2007), "Seismic Assessment of Concentrically Braced Steel Frames with Shape Memory Alloy Braces", *Journal of Structural Engineering*, 10.1061/\_ASCE\_0733-9445\_2007\_133:6\_862, ASCE.
- McCormick J, DesRoches R, Fugazza D, Auricchio F (2006), "Seismic Vibration Control Using Super-elastic Shape Memory Alloys", *Journal of Engineering Materials and Technology*, 128:294-301, The American Society of Mechanical Engineers.
- Motahari S.A, Ghassemieh M, Abolmaali S.A. (2007) "Implementation of Shape Memory Alloy Dampers for Passive Control of Structures Subjected to Seismic Excitations", *Journal of Constructional Steel Research*, 2007; 63:1570\_9. Elsevier Ltd.

Yang W, DesRoches R, Leon RT (2010), "Design and Analysis of Braced Frames with Shape Memory Alloy and Energy-Absorbing Hybrid Devices" *Engineering Structures*, 32:498-507, Elsevier Ltd.